

## **OBJECT-BASED IMAGE ANALYSIS FOR MAPPING FUEL TYPES IN TENERIFE ISLAND USING WORLDVIEW-2 DATA**

A. Alonso-Benito <sup>a\*</sup>, L.A. Arroyo <sup>b</sup>, M. Arbelo <sup>a</sup>, P. Hernández-Leal <sup>a</sup>, L. Núñez-Casillas<sup>a</sup>, L. Arvelo-Valencia<sup>a</sup>

<sup>a</sup> Grupo de Observación de la Tierra y la Atmósfera (GOTA). Departamento de Física FEES, Universidad de La Laguna, 38206 (S/C Tenerife). Spain – aaloben@ull.es

<sup>b</sup> Centro de Investigación del Fuego (CIFU). Fundación General del Medio Ambiente de Castilla-La Mancha, Edificio ICAM de la UCLM (Campus Fábrica de Armas), 45701 Toledo. Spain – Lara.Arroyo@uclm.es

**KEY WORDS:** Forest fuel mapping, WorldView-2, Tenerife Island, object-based image analysis

### **ABSTRACT:**

The aim of this work was to assess the potential of Object-Based Image Analysis for mapping fuel types from WorldView-2 imagery in the Canary Islands (Spain). The study area, located in the north of Tenerife Island, is topographically complex and it includes several endemic species. An adaptation of the Prometheus fuel type to Canary vegetation was mapped from a WorldView-2 image using an object-based image analysis step-wise approach. Then, field data collected during May-December, 2011 was used to validate the obtained classification. The object-based image analysis performed for the WorldView2 imagery produced an overall accuracy of 84%, with most error due to inaccurate of allocation fuel types (allocation disagreement of 11%). Only 5% of the detected disagreement was due to inappropriate proportion of the identified fuel types (quantity disagreement).

---

\* Corresponding author.

## 1. INTRODUCTION

### 1.1 Introduction

Forest fire managers need precise information about the conditions, amount and spatial distribution of forest fuels, since they are key variables in fire behaviour models. Fuel types are defined as the physical characteristics of the live and dead biomasses (fuel elements of distinctive species, form, size arrangement and continuity) that contribute to the spread, intensity and severity of fire (Burgan et al., 1998; Arroyo et al 2008).

Digital fuel maps are a critical input in GIS-based models, which simulate fire behaviour as BEHAVEPlus (fire behaviour prediction and fuel modelling system) (Andrew, 2009), FARSITE (fire area simulator) (Finney, 2004) or FlamMap (fire potential simulator) (Finney, 2006).

Tenerife Island (Canary Islands, Spain), located off the northwest coast of mainland Africa, does not currently have an adequate digital fuel type map. Besides, the presence of endemic species and the complexity of the vegetation of the island results in an unsuitable adjustment of the fuel types defined for the Spanish forests in mainland (MAPA, 1989).

Remotely sensed data provides an important way to derive the spatial distribution of fuel types and its variation over the time, reducing considerably the cost associated to fieldwork. High and medium spatial resolution imagery has proven good performance to map fuel types. Using Quickbird imagery, Arroyo et al (2006), Mutlu et al (2008) and Mallinis et al (2008) obtained fuel type maps with overall accuracies of 81, 76 and 80% respectively. Using ASTER data, Lasaponara and Lanorte (2007) obtained an overall accuracy of 91%.

The objective of this work is to evaluate the potential of using very high spatial resolution WorldView-2 (WV-2) data with an object-based approach (OBIA) to map fuel types in Tenerife Island.

## 2. DATA AND METHODOLOGY

### 2.1 Study area

The study area, with an extension of 18 km<sup>2</sup>, is located in the north of Tenerife Island (Figure 1). The altitude ranges from 870 to 1,808 meters above sea level. It includes a very complex geological mixture of terrains with big ravines. The area contains the most important endemic groups of vegetation in the Canary Islands, being representative of the distinctive vegetation of the Archipelago. Some of most important species included in this region are Azores Laurel (*Laurus azorica* L.), Faya (*Myrica faya* Ait.), Tree Heath (*Erica arborea* L.) or Canary Pine (*Pinus canariensis* L.).

### 2.2 Fieldwork data collection

Field data was collected from 77 circular plots with 10 m radius from May to December of 2011. The plots were located every 500 m, forming a grid that covered the whole study area. The coordinates of the centre of each plot were recorded with a GeoExplorerXT (a minimum of 60 positions were collected for each plot and saved to the GPS unit).

The vegetation species and their heights were collected each meter within four transects starting at the centre of the plot (following North, South, East and West directions). This information was then used to identify the Prometheus fuel types (Prometheus, 2000) adapted to the Canarian vegetation (Table 1). Pots were assigned into one of the following fuel types: M1/M2; M3/M4; M5 and M6/M7 (Figure 2).

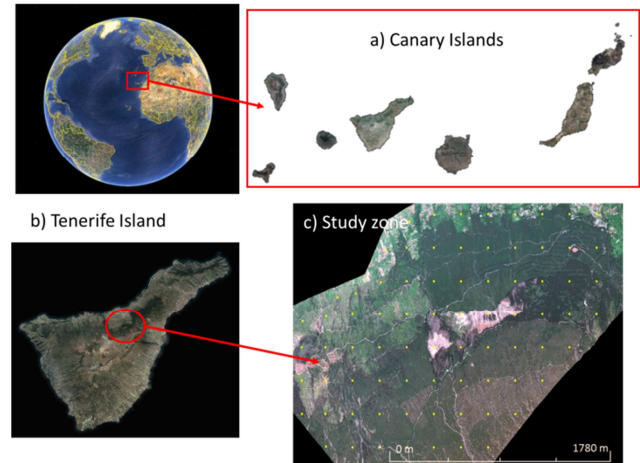


Figure 1. a) and b) orthophoto from GRAFCAN, c) WV-2 image (band combination: RGB 532) of the study area. The yellow dots indicate the location of field plots.

Prometheus Classification	Description	Adapted Prometheus Classification
Fuel type 1 Fuel type 2	grass cover >50% average fuel height 0.3-0.6 m	M1/M2
Fuel type 3 Fuel type 4	average fuel height 0.6-2.0 m average fuel height 2.0-4.0 m	M3/M4
Fuel type 5	shrub cover <30% tree cover >50%	M5
Fuel type 6 Fuel type 7	shrub cover >30%, tree cover >50%, distance between the canopy base and surface fuel layer >0.5 m shrub cover >30%, tree cover >50%, distance between the canopy base and surface fuel layer <0.5 m	M6/M7

Table 1. Prometheus fuel type classification (adapted from Arroyo et al., 2008) and the used fuel type classification (adapted for the Canarian vegetation).

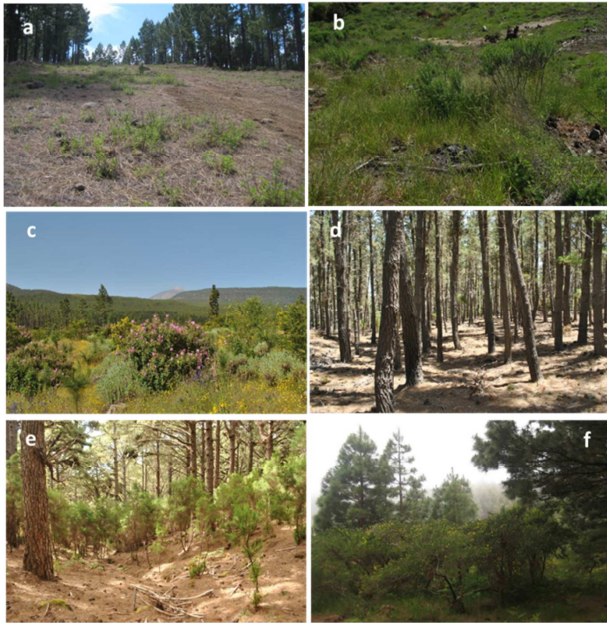


Figure 2. Examples of fuel types within the study area: M1/M2 (a & b), M3/M4 (c), M5 (d) and M6/M7 (e & f).

### 2.3 Satellite data

One WV-2 image of the study area was acquired on June, 2011. The WV-2 sensor provides a very high resolution panchromatic band (0.50 m) and eight multispectral bands (2.00 m), four standard colour (red, green, blue and near-infrared 1) and four new bands (coastal, yellow, red edge and near-infrared 2) (Table 2).

Spectral Band	Centre wavelength (nm)	Sensor Bands (nm)
Panchromatic	632	450 – 800
Coastal	427	400 – 450
Blue	478	450 – 510
Green	546	510 – 580
Yellow	608	585 – 625
Red	659	630 – 690
Red Edge	724	705 – 745
NIR 1	831	770 – 895
NIR 2	908	860 – 1040

Table 2. The spectral information of WV-2 imagery.

The acquired WV-2 image was a standard ortho ready product, which was radiometrically corrected. This image was converted to surface reflectance using the atmospheric correction algorithm/code FLAASH (Fast Line-of-sight Atmospheric Analysis of Spectral Hypercubes) available as a part of ENVI (RSI/ENVITM) image processing package. FLAASH derives its ‘physics based’ mathematics from MODTRAN4 (Cooley et al., 2002).

The resulting image was ortho-rectified using a digital elevation model (DEM) with 5 m spatial resolution. Finally, the image was cropped to the size of the study area.

### 2.4 Vegetation indices

In addition to the original WV-2 image bands, the following vegetation indices were calculated: NDVI (Normalized Difference Vegetation Index) (Rouse et al., 1973); and YNDVI, a modified NDVI where the Yellow and NIR2 Bands are used

instead of the Red and NIR1 Bands. These indices were estimated at an object level.

### 2.5 OBIA classification

The fuel type classification methodology is outlined in Figure 3. First, an iterative multi-scale image segmentation was carried out in order to generate a two-level network of image objects. A level called *vegetation* was created first, and it was used to distinguish the main vegetation groups: coniferous forests and broadleaved forests. In order to reduce the processing time, a thematic band was used to mask out the non-forested areas.

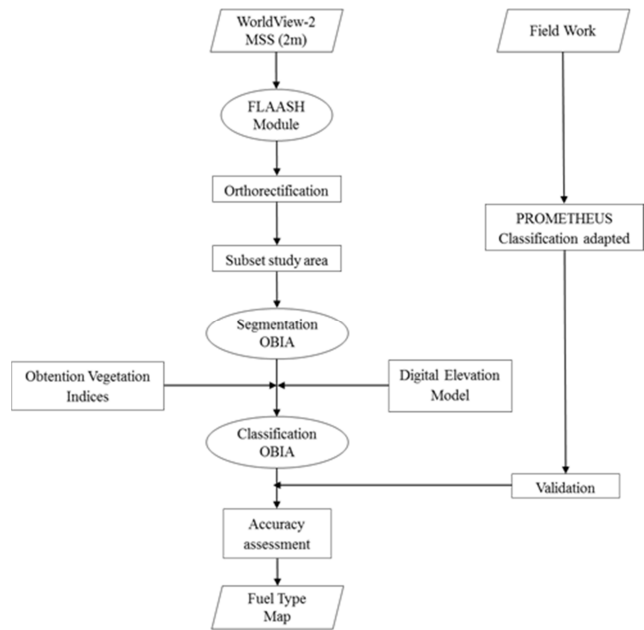


Figure 3. Workflow chart of the methodology used in this study.

The second level, so called *fuel type level*, was segmented using the vegetation indices, the original WR-2 bands and the DEM. The objects created in the fuel type level were classified in a step-wise manner. Those fuel types showing a characteristic spectral behaviour were classified first, and context information was used to aid in the identification of the remaining fuel types. The classification result of level vegetation was considered here by means of hierarchical object-based features. Table 3 shows the object-based features and thresholds used for classifying each fuel type.

Fuel Type	Coniferous	Broadleaved
M1/M2	Mean Coastal $\geq 350$	YNDVI $\leq 0.5$
M3/M4	Mean Yellow $\geq 800$	Mean Blue $\geq 375$
M5	NDVI $\geq 0.7$	Max Diff $\leq 3$
M6/M7	NDVI $\leq 0.55$	No present
	Remaining objects	Remaining objects

Table 3. Object-based features and thresholds used for classifying fuel types

The obtained classification was then refined by re-classifying those small isolated objects that were fully surrounded by a different fuel type. For doing so, we used the feature ‘relative border to’, with a threshold of 1. The obtained map was exported as a shapefile for validation against the field data. The accuracy of the obtained map was estimated by comparison with the 77 plots assessed in the field, using an error matrix.

The performance of the classification was analyzed in terms of error, which was divided in two components: errors due to quantity disagreement and errors due to allocation disagreement (Pontius and Millones, 2011).

### 3. RESULTS AND DISCUSSION

The obtained fuel map is presented in Figure 4. Using OBIA and the spectral information from the WV-2 imagery, four fuel types were identified.

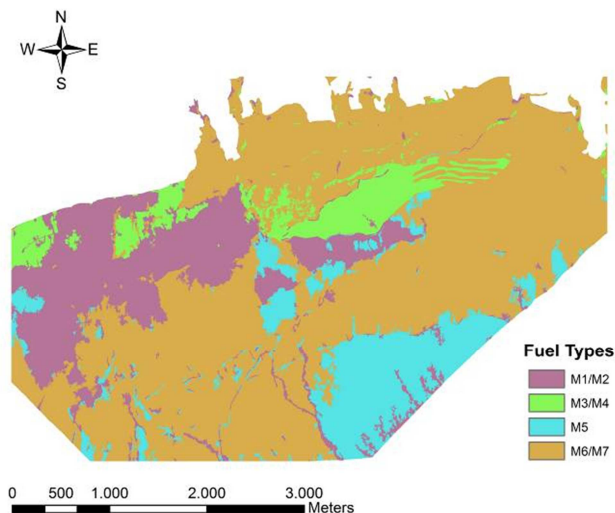


Figure 4. Fuel type map of the study area.

The overall accuracy of the fuel map was 84%. For fuel type M3/M4, 23% of the validation plots had been misclassified as fuel type M6/M7. 12 and 6% of plots assigned as fuel type M6/M7 in the field had been misclassified as fuel types M1/M2 and M3/M4, respectively. Fuel types M1/M2 and M5 were the most accurately classified, with an accuracy of 100%.

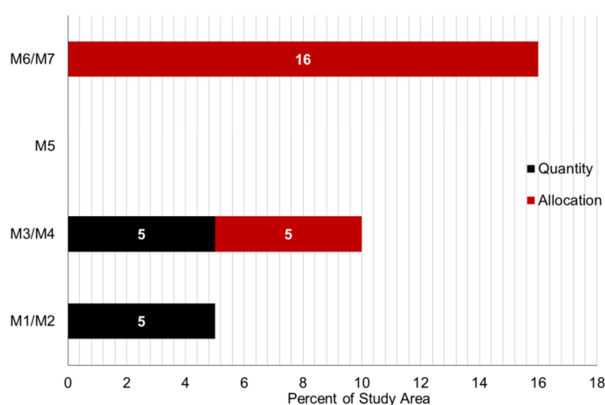


Figure 5. Quantity disagreement and allocation disagreement for each fuel type.

Figure 5 shows proportion of quantity and allocation disagreement for each fuel type. Fuel type M1/M2 showed a quantity disagreement of 5%, whereas fuel type M6/M7 had the highest allocation disagreement (16%). Fuel types M3/M4 showed 5% for quantity and allocation disagreement. Fuel type M5 has not showed any disagreement.

For all the fuel types, the proportion of error assigned to quantity disagreement, indicates differences in the proportion of

fuel types in relation to the proportions found for the validation plots. In contrast, the values obtained for allocation disagreement indicate that, when accurately identified, fuel types were correctly allocated within the study area.

### 4. CONCLUSIONS

Fuel type maps of a topographically complex area can be obtained using OBIA and the spectral information of sensor WV-2.

We are currently studying the possible incorporation of new synthetic indices and LiDAR data to the OBIA. These new sources of information would allow considering the height of the vegetation, which would further improve the developed fuel type mapping method.

### ACKNOWLEDGEMENTS

This work has been supported by PCT-MAC 2007-2013 MAC/1/C055, called SATELMAC Project, co-financed with FEDER funds and by Ministerio de Ciencia e Innovación under grants CGL2010-22189-C02.

### REFERENCES

- Andrews, P.L., 2009. *BehavePlus fire modelling system, version 5.0: Variables*. USDA Forest Service, Rocky Mountain Research Station Gen. Tech. Rep. RMRS-GTR-213 (Fort Collins, CO) pp. 111.
- Alonso-Benito, A., Arroyo, L.A., Arbelo, M., Hernández-Leal, P.A. & González-Calvo, A., 2012. Pixel and object based classification approaches for mapping forest fuel types in Tenerife Island from ASTER data. *International Journal of Wildland Fire*, in revision.
- Arroyo, L.A., Healey, S.P., Cohen, W.B., Cocero, D. & Manzanera, J.A., 2006. Using object-oriented classification and high-resolution imagery to map fuel types in a Mediterranean region. *J. Geophys. Res.* 111(G4), G04S04.
- Arroyo, L., Pascual, C. & Manzanera, J., 2008. Fire models and methods to map fuel types: The role of remote sensing. *Forest Ecology and Management* 256(6), pp. 1239-1252.
- Burgan, R.E., Klaver, R.W. & Klaver, J.M., 1998. Fuel models and fire potential from satellite and surface observations. *International Journal of Wildland Fire*, 8(3), pp. 159-170.
- Cooley, T., Anderson, G.P., Felde, G.W., Hoke, M.L., Ratkowski, A.J., Chetwynd, J.H., Gardner, J.A., Adler-Golden, S.M., Matthew, M.W., Berk, A., Bernstein, L.S., Acharya, P.K., Miller, D., Lewis, P., 2002. FLAASH, a MODTRAN4-based atmospheric correction algorithm, its application and validation. In *Proceeding IEEE International Geoscience and Remote Sensing Symposium, 2002 (IGARSS '02)*. 2002. Volume 3, Issue C, pp. 1414-1418.
- Finney, M.A., 2004. *FARSITE: Fire Area Simulator-model development and evaluation*. USDA Forest Service, Rocky Mountain Research Station Gen. Tech. Rep. RMRS-RP-4 (Ogden, UT) pp. 47.
- Finney, M.A. 2006. *An overview of FlamMap fire modeling capabilities*. In '1st Fire Behavior and Fuels Conference: Fuels management—How to Measure Success', March 27-30 2006,

Portland, Oregon. (Eds. PL Andrews and BW Butler), pp. 213-220.

Huete, A., Didan, K., Miura, T., Rodriguez, E.P., Gao, X., Ferreira, L.G., 2002. Overview of the radiometric and biophysical performance of the MODIS vegetation indices. *Remote Sensing of Environment*, 83(1-2), pp. 195-213.

Kaufman, Y.J. and Tanre, D., 1996. Strategy for Direct and Indirect Methods for Correcting the Aerosol Effect on Remote Sensing: from AVHRR to EOS-MODIS. *Remote Sensing of Environment* 55(1), pp. 65-79.

Lasaponara, R. & Lanorte, A., 2007. Remotely sensed characterization of forest fuel types by using satellite ASTER data. *International Journal of Applied Earth Observation and Geoinformation* 9(3), pp. 225-234.

Mallinis, G., Mitsopoulos, I.D., Dimitrakopoulos, A.P., Gitas, I.Z. & Karteris, M., 2008. Local-Scale Fuel-Type Mapping and Fire Behavior Prediction by Employing High-Resolution Satellite Imagery. *IEEE Journal of Selected Topics in Applied Earth Observations and Remote Sensing*, 1(4), pp. 230-239.

MAPA, 1989. *Clave fotográfica para la identificación de modelos de combustibles*. Ministerio de Agricultura, Pesca y Alimentación, ICONA (Madrid, España).

Merzlyak, M.N., Gitelson, A.A., Chivkunova, O.B. & Rakitin, V.YU., 1999. Non-destructive optical detection of pigment changes during leaf senescence and fruit ripening. *Physiologia Plantarum*, 106(1), pp. 135-141.

Mutlu, M., Popescu, S.C., Stripling, C. & Spencer, T., 2008. Mapping surface fuel models using lidar data and multispectral data fusion for fire behavior. *Remote Sensing of Environment*, 112(1), pp. 274-285.

Penuelas, J., Pinol, J., Ogaya, R., & Filella, I., 1997. Estimation of plant water concentration by the reflectance water index WI (R900/R970). *International Journal of Remote Sensing*, 18(13), pp. 2869-2875.

PROMETHEUS, 2000. *Management techniques for optimization of suppression and minimization of wildfire effects*. System validation. European Commission, DG XII, ENVIR & CLIMATE, ENV4-CT98-0716, 1998-2000 (Ed. CnEVE European Commission).

Pontius, R.G. and Millones, M., 2011. Death to Kappa: birth of quantity disagreement and allocation disagreement for accuracy assessment. *International Journal of Remote Sensing*, 32(15), 4407-4429.

Qi, J., Chehbouni, A., Huete, A.R., Kerr, Y.H. & Sorooshian, S., 1994. A modified soil adjusted vegetation index. *Remote Sensing of Environment* 48(2), pp. 119-126.

Rouse, J.W., Haas, R.H., Schell, J.A. & Deering, D.W., 1973. *Monitoring Vegetation systems in the Great Plains with ERTS*. In 'Third Earth Resources Technology Satellite-1 Symposium', December 1973. (Ed. SC Freden), pp. 309-317.

Updike, T. and Comp, C., 2010. *Radiometric use of WorldView-2 Imagery*. DigitalGlobe, Longmont, Colorado, USA.